Clumping in Hot Star Winds
W.-R. Hamann, A. Feldmeier & L.M. Oskinova, eds.
Potsdam: Univ.-Verl., 2008
URN: http://nbn-resolving.de/urn:nbn:de:kobv:517-opus-13981

Clumping effects on non-thermal particle spectra in massive star systems

A. Reimer
W. W. Hansen Experimental Physics Laboratory & Kavli Institute for Particle Astrophysics & Cosmology, Stanford University, 452 Lomita Mall, Stanford, CA 94305, USA

Observational evidence exists that winds of massive stars are clumped. Many massive star systems are known as non-thermal particle production sites, as indicated by their synchrotron emission in the radio band. As a consequence they are also considered as candidate sites for non-thermal high-energy photon production up to gamma-ray energies. The present work considers the effects of wind clumpiness expected on the emitting relativistic particle spectrum in colliding wind systems, built up from the pool of thermal wind particles through diffusive particle acceleration, and taking into account inverse Compton and synchrotron losses. In comparison to a homogeneous wind, a clumpy wind causes flux variations of the emitting particle spectrum when the clump enters the wind collision region. It is found that the spectral features associated with this variability moves temporally from low to high energy bands with the time shift between any two spectral bands being dependent on clump size, filling factor, and the energy-dependence of particle energy gains and losses.

1 Introduction

Evidence for particle acceleration to relativistic energies mediated by the supersonic winds of massive, hot stars comes from the observation of non-thermal radio emission (e.g., Abbott et al. 1986). This has been interpreted by synchrotron emission on the basis of the measured spectra (much steeper than the canonical value $\alpha_r \sim +0.6$, $F_\nu \propto \nu^{\alpha_r}$) and high brightness temperatures of $\sim 10^{6-7}$K, far exceeding $\sim 10^4$K expected from free-free emission from a steady-state isothermal radially symmetric wind (Wright & Barlow 1975). Those particles has been suggested to be accelerated either in shocks caused by the instability of radiatively driven winds (White 1985), in the shocked wind collision region of multiple systems (e.g., Eichler & Usov 1993) or in the termination shock (Völk & Forman 1982).

Through a statistical study the presence of non-thermal radio emission has been linked to the binarity status of the stellar systems (Dougherty & Williams 2000), which is in support of a scenario where particles being predominantly accelerated at the forward and reverse shocks from the colliding supersonic winds from massive stars. Therefore, in this work I am considering the non-thermal particle spectra from being produced in the collision region of a typical long-period massive binary system.

By now ample evidence has accumulated that hint towards the clumpiness of WR- and O-star winds: non-converging mass loss rates from various methods (thermal radio, H_α, UV-lines, X-ray and IR diagnostics, etc.), polarization and photometric variability, stochastically variable substructures in lines (e.g., Eversberg et al. 1998), the observation of non-thermal radio emission even in some short period binaries (e.g., CygOB2#8A: Blomme 2005) where self-absorption in the optically thick winds should prevent the visibility of a non-thermal component, etc. Still open, however, remains a qualitative assessment about the filling factors, typical clump sizes, clumping startification, etc.

2 Emitting electron spectrum

This work considers, for the first time, the effect of clumpiness in the colliding winds of binary systems on the resulting non-thermal electron spectrum in the collision region at a given orbital phase, assuming that the particles to be accelerated stem from the pool of thermal wind particles. It requires a fully time-dependent treatment of particle injection, acceleration and losses.

For this purpose I describe diffusive particle acceleration and losses (radiatively, and via escape from the collision region with rate T_0^{-1}) that governs the non-thermal emitting electron spectrum, by the kinetic equation:

$$\frac{\partial}{\partial t}N(E,t)+\frac{\partial}{\partial E}\dot{E}\,N(E,t)+\frac{N(E,t)}{T_0}=Q(E,t) \quad (1)$$

where $\dot{E}=aE-\dot{E}_{\rm loss}$, the radiative energy loss rate $\dot{E}_{\rm loss}=(b_{\rm syn}+b_{\rm IC})E^2$ from synchrotron and inverse

Compton losses in the Thomson regime, the acceleration rate $a = \frac{V_{\rm OB}^2(c_r-1)}{3c_r\kappa_{\rm a}}$ (Reimer et al. 2006) with c_r the shock compression ratio, and $\kappa_{\rm a}$ the diffusion coefficient, $T_0 = \frac{r_0}{V}$ the escape time scale for a constant post-shock flow velocity V, and the size of the acceleration region, assumed cylinder-shaped for simplicity, with $r_0 = \kappa_{\rm a}/V$. In this picture the clumpiness of the wind translates into a variable injection rate $Q(E,t)$, while for a homogenuous wind $Q(E,t) \propto \delta(E-E_0)$.

In the following I consider the typical setting of a colliding wind region (see e.g., Eichler & Usov 1993) at a given orbital phase with a clumpy wind of volume filling factor $f_{\rm vol}$ defined as the total volume occupied by the clumps with respect to the total wind volume, $f_{\rm vol} = V_{\rm clump}/V_{\rm tot}$. The simplified picture of a constant particle density within the clump and no particles in the interclump medium used here is sufficient to expose the basic properties of variability in a non-thermal component from a clumpy wind. Furthermore, $f_{\rm vol}$ and $V_{\rm OB}$ shall be constant sufficiently close to the shock region.

$Q(E,t) = Q_0\delta(E-E_0)H(t-t_0)H(t_v-t)$ describes the particle injection into the shock region for a clump of size $l_{\rm clump} = V_{\rm OB}(t_v-t_0)$. The solution is analytic, and shown in Fig. 1 for $t_v \to \infty$. With the spectral index s of the emitting electron spectrum, $\propto E^{-s}$, determined by the acceleration rate and escape, the exponential built-up of the electron spectrum up to a maximum energy $E_c = a/(b_{\rm syn}+b_{\rm IC})$ (see Fig. 2, solid line) is governed by both, energy gains and losses. Steady-state is reached on hours time scale in the typical settings of the colliding wind region in long-period binary systems.

The interclump phase is described by $Q(E,t) \propto E^{-s}\delta(t-t_v)$ as the source term in Eq. 1. For $a > 0$ in this phase the solution of Eq. 1 implies a continued acceleration with the maximum electron energy increasing further exponentially (see Fig. 2, dashed line): the particle acceleration appears as a multi- (here: two)-stage process. For $a = 0$ further acceleration ceases and the emitting electron spectrum declines on typically hour times scales in the astrophysical environment considered here. Variations of the acceleration rate a may be plausible considering that possible variations of the shock conditions (e.g. compression ratio, etc.) as the clumpy winds collide re not unexpected.

Combining injection and interclump phases and taking into account past clump injections into the shock results in a temporally evolving electron spectrum in the wind collision region. An example for $l_{\rm clump} = 10^{12}$cm is shown in Fig. 3. Clearly visible are the spectral features from injection phases, and they propagate from low to high energies as time progresses. Thus the flux variations from clumpy particle injections into the acceleration process in the shock at low energies are anticipated to precede the flux variations at high energies. Ultimately, the underlying physical reason for this time shift is the unavoidable energy dependence of the radiative particle energy losses, and their gains in the acceleration process. In addition to the clump size and volume filling factor, the expected time shift is therefore dependent on the electron energy losses and gains.

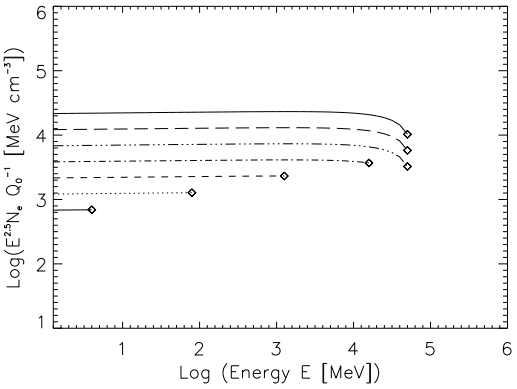

Figure 1: Injection phase: Resulting emitting electron spectrum at times 1, 3, 5, 7, 10, 15 and 20 ksec (correspondingly, lower to upper lines) after $t_0 = 0$ in response to injecting particles into the acceleration process starting at t_0. Parameters used for all figures presented in this work: bolometric luminosity $L_{\rm OB} = 10^6 L_\odot$ and effective temperature $T_{\rm eff} = 45000$K of the star closer to the stagnation point, terminal wind velocities $V_{\rm WR} = V_{\rm OB} = 2000$km/s, mass loss rates of the OB, $\dot{M}_{\rm OB} = 10^{-6}M_\odot$/yr, and WR-star, $\dot{M}_{\rm WR} = 10^{-5}M_\odot$/yr, constant magnetic field in the shock region B=1 G, a stellar separation of $D = 5\cdot 10^{14}$cm, postshock flow velocity $V = 0.6V_{\rm OB}$, diffusion coefficient $\kappa_a = 10^{19}$cm^2/s, shock compression ratio $c_r = 4$ and $E_0 = 1$MeV. Steady-state is reached on hours time scale.

3 Discussion and Outlook

In this work consideration has been given to the effects on the non-thermal electron spectra, as produced in a diffusive shock acceleration process from the pool of thermal wind particles, when the massive star winds are clumped as they collide. In this case, the electron injection into the shock varies with time, dependent on the volume filling factor and typical clump size. Consequently, flux variations are expected in non-thermal particle and photon spectra,

in addition to the thermal emission component. I have shown that those flux variations are expected to appear time shifted when comparing various spectral bands, with the low energy flux variations preceding those at high energies. This clumping signature in non-thermal spectra probes wind clumping in the very vicinity of the collision region, and may possibly show up in multifrequency observations at energy bands that are dominated by non-thermal emission, provided sufficiently dense data sampling.

A metallicity dependence of clumping in non-thermal spectra may be probed by comparing clumping signatures from non-thermal ion spectra, appearing eventually in the gamma-ray domain only through π^0-decay photon emission, with those from non-thermal electron spectra. For this purpose we plan to apply the presented prescription to clumpy ion injections as well.

The presented scenario describes a simplified clumping picture, which nonetheless proves to be sufficient to expose the basic properties of a variable particle injection into the acceleration process in colliding wind regions. This general prescription allows to also account for more complex clumping configurations (e.g. density structure within clump and/or interclump medium, irregular nested clump sizes on various scales, etc.), by modifying the injection term $Q(E,t)$ accordingly.

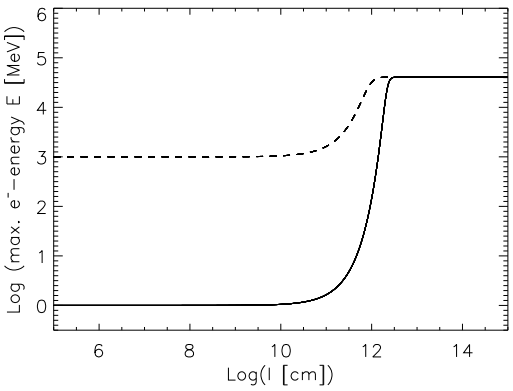

Figure 2: Exponential increase of maximum energy as a function of time with $l = V(t - t_0)$. During the clump injection phase the maximum energy reaches a level $\frac{1}{E_{\mathrm{max},1}(t)} = \frac{1}{E_c} - \left(\frac{1}{E_c} - \frac{1}{E_0}\right) \exp\left(-a\frac{l_{\mathrm{clump}}(t)}{V}\right)$ (solid line). During the interclump phase the maximum particle energy increases further if $a > 0$ as $\frac{1}{E_{\mathrm{max},2}(t)} = \frac{1}{E_c} + \left(\frac{1}{E_{\mathrm{max},1}} - \frac{1}{E_c}\right) \exp\left(-a\frac{l_{\mathrm{interclump}}(t)}{V}\right)$ (dashed line). $E_{\mathrm{max},1} = 10^3$ MeV and the rate of energy gain a =const at all phases is used here for demonstration.

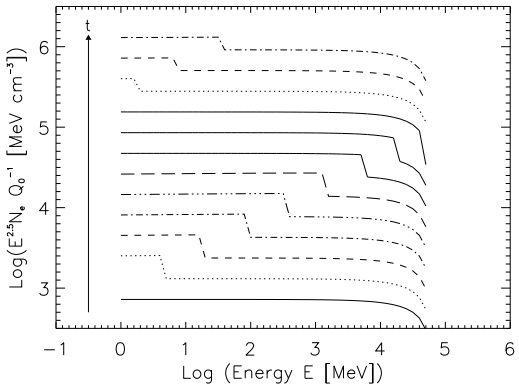

Figure 3: Temporal evolution of the total emitting electron spectrum in the wind collision region with clumpy particle injection and clump size $l_{\mathrm{clump}} = 10^{12}$cm. A temporal step size of Δt = 1ks is used. All spectra are separated artificially in normalization for optimal visibility. a =const at all phases is used here as an example.

References

Abbott, D.C., Bieging, J.H., Churchwell, E. & Torres, A.V. 1986, ApJ, 303, 239

Blomme, R. 2005, Proceedings of "Massive Stars and High-Energy Emission in OB Associations", Liége (Belgium), 2005, Eds. G. Rauw, Y. Nazé, R. Blomme, & E. Gosset, p. 45

Dougherty, S.M. & Williams, P.M. 2000, MNRAS, 319, 1005

Eichler, D. & Usov, V. 1993, ApJ, 402, 271

Eversberg, T., Lepine, S. & Moffat, A.F.J. 1998, ApJ, 494, 799

Reimer, A., Pohl, M. & Reimer, O. 2006, A&A, 644, 1118

Völk, H.J. & Forman, M. 1982, ApJ, 253, 188

White, R.L. 1985, ApJ, 289, 698

Wright, A.E. & Barlow, M.J. 1975, MNRAS, 170, 41

Moffat: Could you not use X-ray light curves of wind-wind collision systems to also probe the clump structure as it makes the X-ray flux flare up as clumps enter the bow shock?

A. Reimer: This should in principle be possible. However, please note that I considered only the non-thermal behaviour of the clumps when they enter the shock. Depending on the X-ray energy band the X-ray flux may however rather be dominated by the thermal hot gas. The resulting thermal spectra when the clumps enter the shock may show different properties than the non-thermal spectra I have been considering here in my talk.

Romero: Anita, can you specify a bit more the physical conditions you are assuming for the clumps? What is the clump density? What is the magnetic field inside the clumps?

A. Reimer: The clump density in my calculations of the non-thermal spectra from the wind-wind collision region as the clumps enter the shock is specified by the variable Q_0. Its value has been left open in the figures shown. The clump size with respect to the volume occupied by the interclump medium is defined via the volume filling factor $f = V_{\rm clump}/V_{\rm tot}$. I used $f = 0.2$ for the examples presented in the figures here. The magnetic field in my calculations is only relevant for the synchrotron losses in the shock region, and its value has been kept constant to 1G for the presented examples. I did not consider any possible interactions of a magnetic field in the clumps with the shock region when clumps enter the shock. This would require MHD calculations.